

Interference effect in elastic parton energy loss in a finite medium

Xin-Nian Wang

Nuclear Science Division, MS 70-319, Lawrence Berkeley National Laboratory, Berkeley, CA 94720 USA
(April 17, 2006)

Similar to the radiative parton energy loss due to gluon bremsstrahlung, elastic energy loss of a parton undergoing multiple scattering in a finite medium is demonstrated to be sensitive to interference effect. The interference between amplitudes of elastic scattering via a gluon exchange and that of gluon radiation reduces the effective elastic energy loss in a finite medium and gives rise to a non-trivial length dependence. The reduction is most significant for a propagation length $L < 4/\pi T$ in a medium with a temperature T . Though the finite size effect is not significant for the average parton propagation in the most central heavy-ion collisions, it will affect the centrality dependence of its effect on jet quenching.

PACS numbers: 12.38.Mh, 24.85.+p; 13.60.-r, 25.75.-q

One of the remarkable phenomena observed in central nucleus-nucleus collisions at the Relativistic Heavy-ion Collider (RHIC) is jet quenching as manifested in the suppression of high transverse momentum hadron spectra [1,2], azimuthal angle anisotropy [4] and suppression of the away-side two-hadron correlations [5]. The observed patterns of jet quenching, their centrality, momentum and colliding energy dependence in light hadron spectra and correlations are consistent with the picture of parton energy loss [6]. However, recent experimental data on measurements of single non-photonic electron spectra [7] seem to indicate a suppression of heavy quarks that is not consistent with the theoretical predictions based on current implementation of heavy quark energy loss [8–10]. This has led to a renewed interest in the elastic (or collisional) energy loss and its effects in the observed jet quenching phenomena [11,12].

Elastic energy loss by a fast propagating parton in general is caused by its elastic scattering with thermal partons in the medium through one gluon exchange. The gluon exchange can be considered as the emission and subsequent absorption of gluons by the two partons and therefore should also be subject to formation time of the virtual gluon due to interference. In a finite medium when the propagation length is comparable to the formation time, the interference should reduce the effective elastic energy loss as compared to an infinite medium. Since the typical energy exchange with a thermal parton is $\omega \sim T$, the average formation time is therefore controlled by the temperature of the medium. In a recent study by Peigne *et al.* [13], however, collisional energy loss was found to be suppressed significantly for considerably large medium size. This might be partially due to the complication of subtraction of induced radiation associated with the acceleration of color charges within a finite period of time in the semi-classical approach.

For partons produced via a hard process that go through further multiple scattering, elastic scattering via one gluon exchange often bears many similarities to the

radiative (or gluon bremsstrahlung) processes. In this paper, we will consider the elastic scattering within the same framework of multiple parton that was employed to study the radiative energy loss [14,15]. We will show that it is the same interference between the amplitudes of elastic scattering and induced radiation that leads to the reduction of the elastic energy loss. Such a reduction gives rise to a non-trivial medium size dependence of the elastic energy loss which approaches the infinite size limit.

For the purpose of illustration and derivation, we start with the double quark scattering processes in deeply inelastic scattering (DIS) off a nucleus and their effects on the nuclear modification of the effective quark fragmentation functions. The differential cross section of semi-inclusive processes $e(L_1) + A(p) \rightarrow e(L_2) + h(\ell_h) + X$ in DIS can be expressed in general as

$$E_{L_2} E_{\ell_h} \frac{d\sigma_{\text{DIS}}^h}{d^3 L_2 d^3 \ell_h} = \frac{\alpha_{\text{EM}}^2}{2\pi s} \frac{1}{Q^4} L_{\mu\nu} E_{\ell_h} \frac{dW^{\mu\nu}}{d^3 \ell_h}, \quad (1)$$

in terms of the semi-inclusive hadronic tensor,

$$E_{\ell_h} \frac{dW^{\mu\nu}}{d^3 \ell_h} = \frac{1}{2} \sum_X \langle A | J^\mu(0) | X, h \rangle \langle X, h | J^\nu(0) | A \rangle \\ \times 2\pi \delta^4(q + p - p_X - \ell_h), \quad (2)$$

and the leptonic tensor, $L_{\mu\nu} = \frac{1}{2} \text{Tr}(\gamma \cdot L_1 \gamma_\mu \gamma \cdot L_2 \gamma_\nu)$, where $q = [-Q^2/2q^-, q^-, \vec{0}_\perp]$ is the four-momentum of the virtual photon, $p = [p^+, 0, \vec{0}_\perp]$ is the momentum of the target per nucleon, $s = (p + L_1)^2$ is the total invariant mass of the lepton-nucleon system, J_μ is the hadronic electromagnetic (EM) current, $J_\mu = e_q \psi_q \gamma_\mu \psi_q$, and \sum_X runs over all possible intermediate states.

The leading-twist contribution to the semi-inclusive hadronic tensor to the lowest order in the strong coupling constant comes from a single virtual photon and quark scattering,

$$\frac{dW_{\mu\nu}^{S(0)}}{dz_h} = \sum_q f_q^A(x) H_{\mu\nu}^{(0)}(x, p, q) D_{q \rightarrow h}(z_h), \quad (3)$$

where $f_q^A(x)$ is the quark distribution in the nucleus, $x = -Q^2/2p^+q^-$ the Bjorken variable, $D_{q \rightarrow h}(z_h)$ the quark fragmentation function and

$$H_{\mu\nu}^{(0)}(x, p, q) = e_q^2 \frac{1}{2p^+q^-} \text{Tr}(\gamma \cdot p \gamma_\mu \gamma \cdot (q + xp) \gamma_\nu) \quad (4)$$

the hard part of $\gamma^* + q$ partonic scattering.

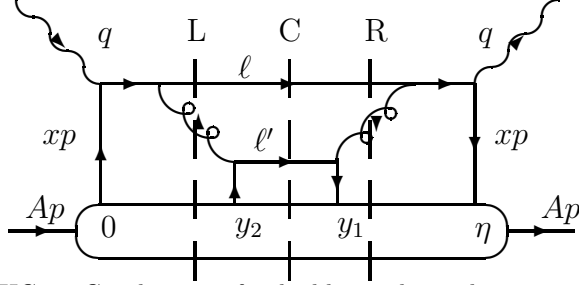


FIG. 1. Cut diagrams for double quark-quark scattering in DIS off a nucleus.

$$T_{qq'}^{A(C)}(x, x_L) = p^+ \int \frac{d\eta^-}{2\pi} dy_1^- dy_2^- e^{i(x+x_L)p^+ \eta^-} (1 - e^{-ix_L p^+ y_2^-}) (1 - e^{-ix_L p^+ (\eta^- - y_1^-)}) \theta(-y_2^-) \theta(\eta^- - y_1^-) \\ \times \langle A | \bar{\psi}_q(0) \frac{\gamma^+}{2} \psi_q(\eta^-) \bar{\psi}_{q'}(y_1^-) \frac{\gamma^+}{2} \psi_{q'}(y_2^-) | A \rangle. \quad (6)$$

is the two-quark correlation function in the nucleus. The four terms with different phase factors in the above matrix element correspond to hard-soft, double hard quark scattering and their interferences, similarly to the Landau-Pomeranchuk-Migdal (LPM) interference in induced gluon radiation [14]. In the hard-soft quark scattering, the first or leading quark that was knocked out of the nucleus by the hard virtual photon becomes off-shell. It then radiates a real gluon which interacts with another soft quark that carries zero fractional momentum (+ component) in the collinear limit (neglecting the initial transverse momentum of the quark) and converts it into the final quark with momentum ℓ' . In this case, the final total longitudinal fractional momentum of the two quarks $x_L = (\ell^+ + \ell'^+)/p^+ = \ell_T^2/2p^+q^-z(1-z)$ comes from the initial leading quark before its interaction with the virtual photon. This kinematics corresponds to the induced emission of a secondary quark like the case of induced gluon radiation. On the other hand, in the process of double hard quark scattering, the leading quark becomes on-shell after its interaction with the vir-

For the simplest case, let us consider multiple scattering between two quarks with different flavors in DIS off a large nucleus as illustrated in Fig. 1 (with the central cut). In this process, a quark (q) knocked out by the virtual photon undergoes a secondary scattering with another quark q' from the nucleus. It contributes to the semi-inclusive DIS at twist four similarly as multiple scattering with gluons in the discussion of induced gluon radiation. We assume the flavors of the two quarks to be different so that there is no contribution from crossing diagrams. The contribution from the central-cut diagram in Fig. 1 to the semi-inclusive tensor is, as given in Ref. [14],

$$\frac{dW_{\mu\nu}^{D(C)}}{dz_h} = \frac{\alpha_s C_F}{2\pi} \int \frac{d\ell_T^2}{\ell_T^2} \int_{z_h}^1 \frac{dz}{z} \left[D_{q \rightarrow h}(z_h/z) \frac{1+z^2}{(1-z)^2} + D_{q' \rightarrow h}(z_h/z) \frac{1+(1-z)^2}{z^2} \right] \\ \times \frac{x_B}{Q^2} \frac{2\pi\alpha_s}{N_C} T_{qq'}^{A(C)}(x, x_L) H_{\mu\nu}^{(0)}(x, p, q), \quad (5)$$

where

tual photon. It then scatters with another quark that carries finite momentum fraction x_L . Therefore, the final total longitudinal fractional momentum of the two quarks x_L is transferred from the initial momentum of the second quark. This is equivalent to elastic scattering between two quarks via one-gluon exchange.

For a complete calculation of double quark scattering processes in DIS, one also has to include interference between triple quark scattering and single quark scattering as given by the left and right cut diagrams in Fig. 1. Their contributions to the semi-inclusive hadronic tensor are very similar to the central-cut diagram,

$$\frac{dW_{\mu\nu}^{D(R,L)}}{dz_h} = \frac{\alpha_s C_F}{2\pi} \int \frac{d\ell_T^2}{\ell_T^2} \int_{z_h}^1 \frac{dz}{z} \left[D_{q \rightarrow h}(z_h/z) \frac{1+z^2}{(1-z)^2} + D_{g \rightarrow h}(z_h/z) \frac{1+(1-z)^2}{z^2} \right] \\ \times \frac{x_B}{Q^2} \frac{2\pi\alpha_s}{N_C} T_{qq'}^{A(R,L)}(x, x_L) H_{\mu\nu}^{(0)}(x, p, q), \quad (7)$$

with the corresponding four-quark matrix elements

$$T_{qq'}^{A(R)}(x, x_L) = p^+ \int \frac{d\eta^-}{2\pi} dy_1^- dy_2^- e^{i(x+x_L)p^+ \eta^-} (-)(1 - e^{-ix_L p^+ y_2^-}) \theta(-y_2^-) \theta(y_2^- - y_1^-) \\ \times \langle A | \bar{\psi}_q(0) \frac{\gamma^+}{2} \psi_q(\eta^-) \bar{\psi}_{q'}(y_1^-) \frac{\gamma^+}{2} \psi_{q'}(y_2^-) | A \rangle, \\ T_{qq'}^{A(L)}(x, x_L) = p^+ \int \frac{d\eta^-}{2\pi} dy_1^- dy_2^- e^{i(x+x_L)p^+ \eta^-} (-)(1 - e^{-ix_L p^+ (\eta^- - y_1^-)}) \theta(y_1^- - y_2^-) \theta(y^- - y_1^-)$$

$$\times \langle A | \bar{\psi}_q(0) \frac{\gamma^+}{2} \psi_q(\eta^-) \bar{\psi}_{q'}(y_1^-) \frac{\gamma^+}{2} \psi_{q'}(y_2^-) | A \rangle. \quad (9)$$

Note the negative signs before the phase factors and the different time orderings as given by the θ functions in the matrix elements from the interference contributions. In addition to the three cut diagrams in Fig. 1, one should also include virtual corrections which correspond to diagrams with cut quark lines right after the virtual photon interaction. The total contribution to the semi-inclusive spectra from double quark scattering should include all three cut diagrams and virtual corrections from which one can then calculate the nuclear modification to the effective fragmentation function due to double quark scat-

tering. The virtual corrections make the total contribution from double quark scattering to the modified fragmentation functions unitary. However, they do not contribute to the quark energy loss we discuss in this paper.

To compute the energy loss experienced by the leading quark due to double quark scattering, one can identify it with the energy fraction the leading quark loses to the second quark in the central-cut diagram or the radiated gluon in the left and right cut diagrams. When summing these contributions, one encounters the combination of the three θ -functions,

$$\int dy_1^- dy_2^- [\theta(-y_2^-) \theta(y_2^- - y_1^-) + \theta(\eta^- - y_1^-) \theta(y_1^- - y_2^-) - \theta(-y_2^-) \theta(\eta^- - y_1^-)] = \int_0^{\eta^-} dy_1^- \int_0^{y_1^-} dy_2^-, \quad (10)$$

which is a path-ordered integral limited by the value of $\eta^- \sim 1/xp^+$. We will neglect any such contact contributions as compared to the dominant contributions whose integration over the location of the second quark is only limited by the size of the nucleus. In this case the two quarks come from two different nucleons in the nucleus and the corresponding contributions are enhanced by $A^{1/3}$ due to the large nuclear size as compared to the

contact contribution. The dominant quark energy loss due to double quark scattering is then

$$\Delta z_{qq} = \frac{\alpha_s^2 C_F}{2N_c} \int \frac{d\ell_T^2}{\ell_T^2} \int dz \frac{1 + (1-z)^2}{zp^+ q^-} \frac{T_{qq'}^A(x, x_L)}{f_q^A(x)}, \quad (11)$$

where the four-quark matrix element $T_{qq'}^A(x, x_L)$ is defined as

$$T_{qq'}^A(x, x_L) = p^+ \int \frac{d\eta^-}{2\pi} dy_1^- dy_2^- e^{ix_L p^+ \eta^- + ix_L p^+ (y_2^- - y_1^-)} (1 - e^{-ix_L p^+ y_2^-}) \theta(-y_2^-) \theta(\eta^- - y_1^-) \times \langle A | \bar{\psi}_q(0) \frac{\gamma^+}{2} \psi_q(\eta^-) \bar{\psi}_{q'}(y_1^-) \frac{\gamma^+}{2} \psi_{q'}(y_2^-) | A \rangle. \quad (12)$$

One can notice that the above matrix element has an overall phase factor $e^{ix_L p^+ (y_2^- - y_1^-)}$ as a consequence of the cancellation by the interference processes in the left and right cut diagrams. Therefore, the remaining contribution from the double quark scattering requires the second quark to carry initial longitudinal momentum $x_L p^+$ that provides the total longitudinal momentum of the final quarks after the elastic scattering between the leading and the second quark. The above contributions also contain the interference between elastic and radiative amplitudes in which the leading quark first emits a real gluon (or close to real if the initial transverse momentum is not neglected) which converts a soft quark into the final quark with momentum ℓ' .

To a good approximation, especially for the application to the case of parton propagation in the dense medium in heavy-ion collisions, we can neglect the correlation between the initial leading quark and the secondary quark in the nuclear medium. The above matrix element can be factorized as a product of the leading quark $f_q^A(x)$ and the secondary quark distribution in the medium. In the rest frame of the nuclear medium, we have

$$\frac{T_{qq'}^A(x, x_L)}{f_q^A(x)} = 2\pi \int dy \rho(y) f_{q'}(x_L) \left[1 - e^{i \frac{\ell_T^2}{2Ez(1-z)} y} \right], \quad (13)$$

where $y = (y_1 + y_2)/2$, $f_{q'}(x_L)$ is the secondary quark distribution per nucleon and $\rho(y)$ is the spatial profile of the nucleus.

One can extend the above calculation to quark propagation in a hot medium in high-energy heavy-ion collisions. For the scattering between a leading quark with energy E and a thermal quark with energy ω that is a basic constituent of the medium, the quark distribution in a thermal medium with temperature T is,

$$\rho_q(y) f_q(x_L) = d_q \int \frac{d\omega}{2\pi^2} \frac{\omega^2}{e^{\omega/T} + 1} \delta(x_L - 1), \quad (14)$$

where $x_L = \ell_T^2/2\omega E z(1-z)$, d_q is the number of degrees of degeneracy for the quark and the spatial dependence is explicitly through the temperature $T(y)$. One can complete the integration over z and ℓ_T in Eq. (11). The corresponding elastic energy loss is then

$$\Delta z_{qq} = \frac{C_F}{N_c} \pi \frac{\alpha_s^2}{E} d_q \int dy \int \frac{d\omega}{2\pi^2} \frac{\omega}{e^{\omega/T} + 1} [1 - \cos(\omega y)] \times \left[2 \ln \frac{1 + \chi_\omega}{1 - \chi_\omega} - \frac{9}{4} \chi_\omega + \frac{3}{8} \chi_\omega^2 \right], \quad (15)$$

where $\chi_\omega = \sqrt{1 - 2\mu^2/\omega E}$ and μ is the Debye screening mass which regularizes the collinear divergence normally associated with parton radiation or small angle scattering. A more consistent treatment is to use a fully resummed gluon propagator in the finite temperature field theory as in previous studies [16]. With the above equation, one can calculate the elastic energy loss for any spatial profile $T(y)$ of the thermal medium. To simplify the calculation, we neglect the thermal fluctuation of the quark energy in the variable χ_ω and replace ω with $3T$. One can carry out the thermal averaging and obtains,

$$\Delta z_{qq} = \frac{C_F}{N_c} \pi \frac{\alpha_s^2}{E} \int dy \frac{\rho_q(T)}{2T\eta(3)} [\eta(2) - \text{Re} \eta(2, iyT)] \times \left[2 \ln \frac{1 + \chi_T}{1 - \chi_T} - \frac{9}{4} \chi_T + \frac{3}{8} \chi_T^2 \right], \quad (16)$$

where

$$\eta(s, a) \equiv \sum_{n=1}^{\infty} \frac{(-1)^{n-1}}{(n+a)^s}; \quad \eta(s) \equiv \eta(s, 0), \quad (17)$$

and $\rho_q(T) = d_q \eta(3) T^3 / \pi^2$ is the local thermal quark density and $\chi_T = \sqrt{1 - 2\mu^2/3TE}$.

One can similarly consider quark energy loss due to elastic quark-gluon scattering which is more involved. In particular, the quark-gluon Compton scattering processes are very similar to the induced gluon

bremsstrahlung as considered in previous studies of radiative energy. As we will show in a separate study [17], the original result [14] for radiative parton energy loss actually contains both radiative and elastic processes. The LPM interference is in fact the interference between the radiative and elastic scattering amplitudes that are also responsible for the interference effects in the elastic energy loss in this paper. The final result for the elastic energy loss due to quark-gluon scattering is

$$\Delta z_{qg} = \frac{C_A}{N_c} \pi \frac{\alpha_s^2}{E} \int dy \frac{\rho_g(T)}{2T\zeta(3)} [\zeta(2) - \text{Re} \zeta(2, iyT)] \times \left[3 \ln \frac{1 + \chi_T}{1 - \chi_T} - \chi_T \right], \quad (18)$$

where

$$\zeta(s, a) \equiv \sum_{n=1}^{\infty} \frac{1}{(n+a)^s}; \quad \zeta(s) \equiv \zeta(s, 0), \quad (19)$$

and $\rho_g(T) = d_g \zeta(3) T^3 / \pi^2$ is the local thermal gluon density. Note that $\eta(2) = \zeta(2)/2$, $\eta(3) = (3/4)\zeta(3)$, $\zeta(2) = \pi^2/6$ and $\zeta(3) \approx 1.2021$.

For the simplest parton density profile, we consider a finite medium with a constant parton density and a length L . The spatial integrations in the above elastic energy loss can be carried out. The total elastic energy losses are ($dE/dL = \Delta E/L$)

$$\frac{dE_{qq}}{dL} = \frac{C_F}{N_c} \frac{\pi \alpha_s^2}{24} d_q T^2 \left\{ 1 - \frac{6}{\pi TL} \left[\frac{1}{\pi TL} - \text{cosec}(\pi TL) \right] \right\} \left[2 \ln \frac{1 + \chi_T}{1 - \chi_T} - \frac{9}{4} \chi_T + \frac{3}{8} \chi_T^2 \right], \quad (20)$$

$$\frac{dE_{qg}}{dL} = \frac{C_A}{N_c} \frac{\pi \alpha_s^2}{12} d_g T^2 \left\{ 1 - \frac{3}{\pi TL} \left[\text{cth}(\pi TL) - \frac{1}{\pi TL} \right] \right\} \left[3 \ln \frac{1 + \chi_T}{1 - \chi_T} - \chi_T \right], \quad (21)$$

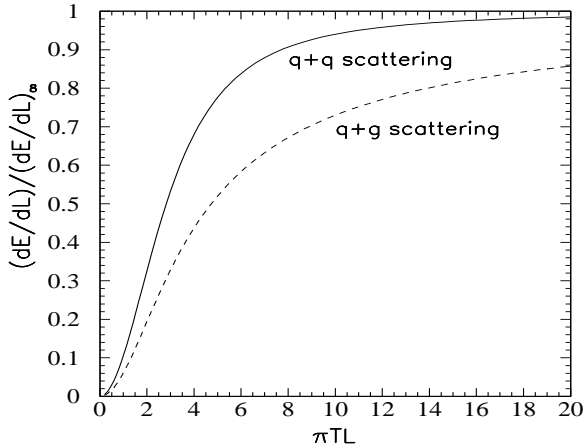


FIG. 2. Elastic energy loss in a finite size thermal medium (at temperature T) dE/dL as a function of the medium length L normalized to the asymptotic value $(dE/dL)_\infty$ for $L = \infty$.

For a medium with infinite length $L \rightarrow \infty$, the above elastic energy losses have finite asymptotic values,

$$\left(\frac{dE_{qa}}{dL} \right)_\infty = \left\langle \frac{\rho_a}{2\omega} \int_{\mu^2}^{\omega E/2} d\ell_T^2 \frac{d\sigma_{qa}}{d\ell_T^2} \ell_T^2 \right\rangle, \quad (a = q, g), \quad (22)$$

which can be interpreted as the average energy transfer $\nu = \ell_T^2/2\omega$ per mean-free path $\lambda_{qa} = 1/\rho_a \sigma_{qa}$ [18] due to elastic scattering between the leading quark and thermal partons. Here $d\sigma_{qa}/d\ell_T^2$ is the differential cross section for $q + a$ elastic scattering.

One can observe from the above results that the effective elastic energy loss for a quark propagating in a medium with a finite length L is reduced from its asymptotic value due to the interference between the elastic and radiative amplitudes. The underlying physics is very similar to the LPM interference in the gluon bremsstrahlung induced by multiple scattering. In the elastic scattering, the gluon exchange can be considered as the gluonic field built up around the propagating quark over finite period of time. The formation time in the case of elastic scattering with thermal partons is controlled by the thermal energy of the partons and therefore is determined by the temperature on the average. Shown in Fig. 2 is the quark elastic energy loss dE_{qa}/dL ($a = q, g$) due to quark-quark and quark-gluon scattering normalized to the asymptotic

value $(dE_{qa}/dL)_\infty$ ($a = q, g$) in a finite medium as a function of a dimensionless variable πTL . The dependence on L is the strongest when $\pi TL \ll 1$,

$$\frac{dE_{qq}}{dL} \approx \frac{7}{60}(\pi TL)^2 \left(\frac{dE_{qq}}{dL} \right)_\infty \quad (23)$$

$$\frac{dE_{gg}}{dL} \approx \frac{1}{15}(\pi TL)^2 \left(\frac{dE_{gg}}{dL} \right)_\infty. \quad (24)$$

When $L \rightarrow 0$, the destructive interference becomes complete and the elastic energy loss vanishes.

The typical average propagation length of a parton in the most central $Au + Au$ collisions is about $L \sim 6$ fm. For an average temperature $T \sim 200 - 300$ MeV, $\pi TL \sim 19 - 28$. In this case the interference effect is quite small as seen in Fig. 2. This is quite different from the results in Ref. [13]. However, for partons produced in the peripheral region of heavy-ion collisions whose propagation length is on the order of 1-2 fm, the reduction of the elastic energy loss due to interference is still significant. For an accurate and consistent treatment of elastic energy loss, one should take into account the interference effect and the non-trivial distance dependence. For an expanding system with a realistic parton density profile, one has to numerically compute the elastic energy loss and the corresponding modified fragmentation functions according to Eq. (15). Furthermore, one should also treat radiative and elastic energy loss in the same framework since there is intricate connection between the two. This will be discussed in a separate work [17].

Note added: After completion of this paper, the author noticed a recent publication [19] in which the finite size effect on elastic energy loss is a result of the imposed finite interaction time which modifies the energy conservation and therefore the phase space available for final partons after elastic scattering. The interference effect discussed in the current paper is not included and therefore the obtained length and energy dependence of the elastic energy loss are different.

The author would like to acknowledge useful discussions with M. Djordjevic and M. Gyulassy at the end of 2005 during the write-up of this manuscript. He also thanks S. Peigne for reading and comments on the manuscript. This work is supported by the Director, Office of Energy Research, Office of High Energy and Nuclear Physics, Divisions of Nuclear Physics, of the U.S. Department of Energy under Contract No. DE-AC02-05CH11231.

-
- [1] K. Adcox *et al.*, [PHENIX Collaboration], Phys. Rev. Lett. **88**, 022301 (2002) [arXiv:nucl-ex/0109003]; S. S. Adler *et al.*, [PHENIX Collaboration], Phys. Rev. Lett. **91**, 072301(2003) [arXiv:nucl-ex/0304022].
 - [2] C. Adler *et al.* [STAR Collaboration], Phys. Rev. Lett. **89**, 202301 (2002) [arXiv:nucl-ex/0206011];
 - [3] J. Adams *et al.* [STAR Collaboration], Phys. Rev. Lett. **91**, 172302 (2003) [arXiv:nucl-ex/0305015].
 - [4] C. Adler *et al.* [STAR Collaboration], Phys. Rev. Lett. **90**, 032301 (2003) [arXiv:nucl-ex/0206006].
 - [5] C. Adler *et al.*, [STAR Collaboration], Phys. Rev. Lett. **90**, 082302 (2003) [arXiv:nucl-ex/0210033].
 - [6] X. N. Wang, Phys. Lett. B **595**, 165 (2004) [arXiv:nucl-th/0305010].
 - [7] S. S. Adler *et al.* [PHENIX Collaboration], Phys. Rev. Lett. **96**, 032301 (2006) [arXiv:nucl-ex/0510047].
 - [8] M. Djordjevic and M. Gyulassy, Phys. Lett. B **560**, 37 (2003) [arXiv:nucl-th/0302069].
 - [9] N. Armesto, M. Cacciari, A. Dainese, C. A. Salgado and U. A. Wiedemann, arXiv:hep-ph/0511257.
 - [10] H. van Hees, V. Greco and R. Rapp, Phys. Rev. C **73**, 034913 (2006) [arXiv:nucl-th/0508055].
 - [11] M. G. Mustafa, Phys. Rev. C **72**, 014905 (2005) [arXiv:hep-ph/0412402].
 - [12] S. Wicks, W. Horowitz, M. Djordjevic and M. Gyulassy, arXiv:nucl-th/0512076.
 - [13] S. Peigne, P. B. Gossiaux and T. Gousset, arXiv:hep-ph/0509185.
 - [14] X. F. Guo and X.-N. Wang, Phys. Rev. Lett. **85** (2000) 3591 [arXiv:hep-ph/0005044]; X.-N. Wang and X. F. Guo, Nucl. Phys. A **696**, 788 (2001) [arXiv:hep-ph/0102230].
 - [15] B. W. Zhang and X. N. Wang, Nucl. Phys. A **720**, 429 (2003) [arXiv:hep-ph/0301195]; B. W. Zhang, E. Wang and X. N. Wang, Phys. Rev. Lett. **93**, 072301 (2004) [arXiv:nucl-th/0309040]; Nucl. Phys. A **757**, 493 (2005) [arXiv:hep-ph/0412060].
 - [16] M. H. Thoma and M. Gyulassy, Nucl. Phys. B **351**, 491 (1991); Phys. Rev. D **44**, 2625 (1991).
 - [17] X.-N. Wang, to be published.
 - [18] X. N. Wang, Phys. Rept. **280**, 287 (1997) [arXiv:hep-ph/9605214].
 - [19] M. Djordjevic, arXiv:nucl-th/0603066.